**International Global Navigation Satellite Systems Association**
**IGNSS Conference 2016**

Colombo Theatres, Kensington Campus, UNSW Australia
6 – 8 December 2016

# Cooperative P2I localization using UWB and Wi-Fi

***Salil Goel***
Joint PhD Student (MIPP Scholar)
Department of Infrastructure Engineering,
The University of Melbourne, Australia
And
Department of Civil Engineering,
Indian Institute of Technology Kanpur, India
Ph: +61-0431740105,
Email: goel.salilg@gmail.com

***Allison Kealy***
Associate Professor
Department of Infrastructure Engineering,
The University of Melbourne, Australia
Email: a.kealy@unimelb.edu.au

***Guenther Retscher***
Associate Professor
Department of Geodesy and Geoinformation,
TU Wien, Vienna, Austria
Email: guenther.retscher@tuwien.ac.at

***Bharat Lohani***
Professor
Department of Civil Engineering,
Indian Institute of Technology Kanpur, India
Email: blohani@iitk.ac.in

## ABSTRACT

A Peer to Infrastructure (P2I) cooperative localization system makes use of existing infrastructure network for localization of mobile platforms. This interconnected network can be utilized for several applications besides communication such as disaster management, situational awareness, search and rescue, guided navigation, Cooperative Intelligent Transport System etc. The focus of this paper is development and analysis of a localization system using a well-established infrastructure network. This paper develops methods of localization of dynamic platforms such as Unmanned Aerial Vehicles (UAV) equipped with GNSS, inertial sensors (INS), ultra-wide band (UWB) and wireless local area network (Wi-Fi) receivers. Traditional platforms (cars, UAVs etc.) rely on GNSS for accurate localization and thus cannot be used in indoor environments or other GNSS challenging regions. This paper leverages continuously deployed networks of urban infrastructure that provide signals of opportunity such as Wi-Fi, as well as UWB to develop a robust localization system which is capable of providing a continuous and seamless position solution in both indoor and outdoor environments. This paper also provides an analysis of this localization system using numerical simulations and discusses experimental results of a

developed prototype. The contributions of this paper include development and analysis of a prototype cooperative localization system and quantification of its performance. Initial simulation results show that in GNSS denied regions, a platform may be able to achieve positioning accuracy comparable to the accuracy provided by a GNSS under certain conditions. In GNSS available regions, other signals further improve the solution obtained using only GNSS. The simulation results are validated using experiments and the developed system achieves an accuracy of better than 10m more than 95% of the time using a maximum of 4 UWB measurements when GNSS is not present at all and more than 3 UWB measurements are available only 2.5% of time. Higher localization accuracy can be achieved using dense infrastructure network and better quality of UWB measurements.

**KEYWORDS**: Cooperative Localization, Extended Kalman Filter, Ultra-Wide Band (UWB), Multi sensor fusion.

## 1. INTRODUCTION

According to a report by United Nations (UN) and World Health Organization (WHO), as of 2014, about 54% of the world's population is living in urban areas and is expected to increase to 66% by 2050 (UN Report 2014). The urban population in the world has been growing rapidly from 746 million in 1950 to 3.9 billion in 2014. This means that a larger number of people are moving to urban areas thus resulting in a significant expansion of the urban regions. Such an expansion is expected to result in dense urban canyons and thus making navigation in urban regions even more challenging. Global Navigation Satellite System (GNSS) which has been the primary mode of navigation is unlikely to cater to the challenging requirements posed by the increasing urban canyons. To tackle the challenges of growing urban canyons, new navigation solutions are required which can operate independent of GNSS and provide navigation solution in cases when GNSS is not available. These new solutions may provide additional information when GNSS is present resulting in improved navigation.

To cater to the needs to increasing urban population, the governments generally put in a lot of investment in developing the infrastructure such as telephone towers, Wi-Fi hotspots etc. This existing infrastructure may prove to be helpful for navigation in urban canyons. Recent literature has demonstrated that navigation may be achieved using signals such as Wi-Fi and GSM (Global signal for mobile communication) (Schauer et al. 2013, Retscher andTatschl 2016) which were originally intended for communication only and are readily available are used in all urban regions. Another recent radio technology called Ultra-Wide Band (UWB) has demonstrated interesting results for navigation in challenging regions (Goel et al. 2016a). The new solutions for navigation can utilize this existing infrastructure and ever increasing web of signals to achieve precise navigation both in GNSS present and GNSS denied regions. This paper refers to the navigation using signals from existing infrastructure as cooperative navigation.

Cooperative navigation of a dynamic platform (referred to as 'peer') such as cars, trucks, unmanned aerial vehicle etc. using signals from infrastructure is referred to as Cooperative Peer to Infrastructure (P2I) navigation. Thus cooperative P2I aims to leverage the existing infrastructure and signals for navigation especially in GNSS challenging regions. Upcoming technologies such as Cooperative Intelligent Transport Systems (CITS), Driverless cars and Internet of Things (IoT) are all based on cooperative P2I systems. A cooperative P2I system can provide a reliable, consistent and robust navigation solution under all environments

(indoor and outdoor) irrespective of the availability of GNSS. This is tremendously useful in applications such traffic management, emergency response, disaster management and situational awareness. Navigation in indoor environments and GNSS challenging regions such as tunnels can be achieved easily using cooperative P2I systems.

Cooperative localization for dynamic platforms has been mostly limited to Peer to Peer (P2P) systems (Bailey et al. 2011, Shi et al. 2013, Li and Nashashibi 2013, Wanasinghe et al. 2014, Goel et al. 2016a). This is especially due to the reason that P2P system can be readily deployed under all circumstances and are not dependent on the availability of the infrastructure. Further, deployment of a P2I localization system is generally more expensive than a P2P system and requires more infrastructure, maintenance, time and effort (Goel et al. 2016b). However, P2I systems offer better reliability and accuracy compared to a P2P system. Hence P2I systems are more suitable to be implemented on a larger scale where accuracy requirements are generally difficult to meet.

The focus of literature has been on distributed systems for cooperative localization due to distributed systems being more adaptable and robust. Also compared to centralized systems, distributed systems are less computationally expensive. However, the ease in computational complexity in distributed systems is achieved at the cost of decreased localization accuracy (Goel et al. 2016b). Furthermore, a major challenge in distributed systems has been computation of correlations among the states of nodes which poses additional hurdles towards achieving precise localization and may even cause solution to diverge (Li and Nashashibi 2013, Wanasinghe et al. 2014, Julier and Uhlmann 1997). In an attempt to develop distributed systems, a number of algorithms have been attempted in literature including Unscented Kalman Filter (Shi et al. 2013), Covariance Intersection (Julier and Ulhmann 1997, Hlinka et al. 2014. Carrillo-Arce et al. 2013), Split Covariance Intersection (Li and Nashashibi 2013, Wanasinghe et al. 2014), and Belief Propagation (Chen et al. 2013, Savic and Zazo 2013, Wan et al. 2014). All the above mentioned distributed approaches are aimed at computing unknown correlations and precise localization. However, methods such as covariance intersection and split covariance intersection require explicit computation of states of other nodes and cannot be implemented in the presence of only range measurements (Goel et al. 2016a). Belief propagation on the other hand is computationally expensive, works only on tree networks and may diverge in case of loopy networks, which is generally the case in cooperative networks (Goel et al. 2016a, Savic et al. 2010). A P2I system is inherently distributed in nature and can achieve accuracies comparable to a centralized system at the cost of computational burden equivalent to distributed systems. Thus a P2I system is inherently free from problems such as unknown correlations and failure in loopy networks making it an ideal choice for high precision applications such as mapping etc.

This paper develops a cooperative P2I localization system for dynamic platforms equipped with GNSS and inertial sensors such as gyroscopes and accelerometers. Additional sensors such as UWB and Wi-Fi receivers are also installed on the platform. Further this paper analyses the performance of a P2I localization system with respect to different parameters such as availability of various signals like GNSS, Wi-Fi and UWB and contribution of different signals to the accuracy of the system. Section 2 presents the mathematical models to compute time of flight (TOF) measurements from UWB and Wi-Fi signals and trilateration methods to achieve localization for a static system using range measurements derived from TOF. Section 3 introduces the dynamics of the platform and presents details regarding inclusion of observations from gyroscopes, accelerometers and pseudorange measurements from GNSS whenever available. The later part of section 3 presents a full cooperative P2I system for a dynamic platform by including measurements from all signals like GNSS, UWB, Wi-Fi and observations from gyroscopes and accelerometers. Section 4 presents the results of the numerical simulation and analyses the performance of a P2I system under different

scenarios. The second part of section 4 presents a brief introduction of a prototype of a P2I localization system developed at The University of Melbourne and discusses the results of a preliminary experiment performed using this prototype. The conclusions and future work of this paper is presented in section 5.

## 2. LOCALIZATION USING Wi-Fi AND UWB

This section presents the mathematical models of achieving localization using Ultra-Wide Band (UWB) signals and Wi-Fi. A number of ways of estimating location using Wi-Fi either based on received signal strength (RSS) or TOF have been demonstrated in the literature. This section first discusses different ways of localization using Wi-Fi and then decides on the appropriate mode of Wi-Fi localization. The later part of this section demonstrates the use of relative range measurements from three or more UWB/Wi-Fi transmitters to achieve localization using trilateration methods.

Traditional methods of Wi-Fi localization rely on the method of Wi-Fi fingerprinting (Retscher and Tatschl 2016, Xiao et al. 2011, Mok and Retscher 2007, Husen and Lee 2014). Wi-Fi fingerprinting methods use Received Signal Strength Indicator (RSSI) of all the access points (APs) in the coverage to determine the user location. The location fingerprinting method using Wi-Fi generally involves two phases: training phase and positioning phase. The training phase which is a very important step in location fingerprinting requires a receiver to scan the environment periodically and record the RSS of all the APs in the vicinity. The RSS scans are measured at known reference points which are generally distributed throughout the region of interest which define the `fingerprint' on a particular reference point. After the completion of the training phase, the collected RSS data is processed to build a map and is stored in a database (Retscher and Tatschl 2016). The positioning phase utilizes this database to determine the location of the user. This is done by collecting the RSS of the APs in real time and comparing it with the recorded RSS map stored in the database. To establish the relationship between the RSS and the distance, a number of path loss models have been developed over the years. The distance values can be computed from RSS estimates using a radio wave propagation model. One such model relating RSS and distance is given by the following equation (Retscher and Tastchl 2016).

$$PL(d) = PL(d_o) + 10\gamma \log\left(\frac{d}{d_o}\right) + q, \quad d \geq d_o \geq d_f \qquad \text{(Eq. 1)}$$

Where $PL(d)$ denotes the path loss at distance $d$ between the transmitter and receiver in dB, $d_o$ is the reference distance and $d_f$ denotes the Fraunhofer distance. The notation $\gamma$ is called path loss exponent and describes the slope of average increase in path loss with distance (Retscher and Tatschl 2016). The parameter $q$ incorporates reflection, diffraction and scattering for both LOS and NLOS (Non line of sight) path. The parameter $q$ is a random variable from a zero-mean normal distribution with standard deviation $\sigma$. The authors in Retscher and Tatschl 2016 have developed a differential approach using Wi-Fi termed as DWi-Fi which is based on a principle similar to Differential GPS (DGPS). Other ways of establishing relationship between RSS and distance is to use regression models (Retscher et al. 2012). However, both these methods are time consuming and labour intensive and are thus not feasible for larger areas such as a city with multiple Wi-Fi hotspots. Further, RSS measurements are governed by changes in the environment, movement of people/cars/objects etc. and thus RSS based methods are not suitable for highly dynamic environments such as cities. Neither path loss models nor regression based models are suitable due to the high dynamic nature of the cities. An alternative approach for Wi-Fi positioning is to use range measurements derived from TOF for Wi-Fi (Schauer et al. 2013, Lanzisera et al. 2011). A

number of TOF approaches for Wi-Fi have been attempted in the literature such as time difference of arrival (TODA) (Li et al. 2000, Yamasaki et al. 2005), hybrid combination of TOF and RSS (Abusubaih et al. 2007), angle of arrival (AOA) technique with MIMO compatible APs (Wong et al. 2008), TOF determination using NULL-ACK sequences (Schauer et al. 2013). Most of the methods focus on two way TOF techniques so as to avoid complex time synchronization issues between APs and Wi-Fi receiver. The distance between receiver and APs can be computed from TOF using the following equation (Schauer et al. 2013).

$$d = \frac{c\left(RTT - t_{PROC\_AP}\right)}{2} \qquad \text{(Eq. 2)}$$

Where $RTT$ is called round-trip time and is the same as two way TOF, $t_{PROC\_AP}$ denotes the processing time of signal at the Aps and $c$ denotes the speed of light. A number of RTOF (round-trip TOF) methods have been investigated in the literature, a review of which is given in Schauer et al. 2013. In one of the most recent methods, authors in Schauer et al. 2013 use NULL-ACK frames to compute RTT which is converted to distance measurements after a calibration procedure. They demonstrated that it may be possible to achieve a distance measurement accuracy of about 1.33 metres using a band bass filter and average of large number of RTT measurements in a relatively obstruction free environment. However, they also observed that the mean deviation of the measured range is always more than about 5-6 metres and thus concluded that current systems are not capable of achieving higher accuracy. The new IEEE 802.11v standard includes a more accurate TOF based measurement system and thus may be more suitable for TOF based localization using Wi-Fi (Schauer et al. 2013).

Localization using UWB is based on determination of TOF which is rather straightforward compared to Wi-Fi. Commercially available UWBs such as 'Time Domain P410' UWB rely on two way TOF to realize the distance between the UWBs. To determine relative range using a two way TOF, the UWB system uses a master-slave relationship among the UWBs. The master (transmitter) UWB sends a command to the slave UWB. The slave UWB receives this signal from the master and responds back. The master UWB computes the time taken to receive the signal back which is referred to as TOF. A graphical depiction of the measurement of two way TOF by a master UWB to the slave UWB is shown in Figure 1.

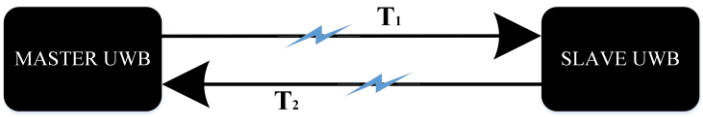


**Figure 1: Measurement of TOF in UWB.**

The relative range can thus be directly derived from two way TOF measurements from UWB as given by the following equation.

$$range = \frac{c\left(t_1 + t_2\right)}{2} \qquad \text{(Eq. 3)}$$

Accurate measurement of relative range between the UWBs is governed by a number of factors including accurate measurement of TOF which depends on system clock accuracy and multipath mitigation. Time domain claims to have a system clock accuracy of less than 10 ps resulting in a precise range measurement. UWBs can detect and remove multipath errors due to the use of wide bandwidth of radio frequency used. The radio frequency (RF) pulse transmitted by the UWB has a bandwidth of about 2 GHz resulting in a physical pulse length of about 15 cm (Petroff 2012). Due to the length of pulses being small, it is possible to separate them and thus reflections resulting from multipath can be resolved from the main

signal by using the first arriving pulse. The multipath effect and received waveform in a cluttered environment is demonstrated in Figure 2.

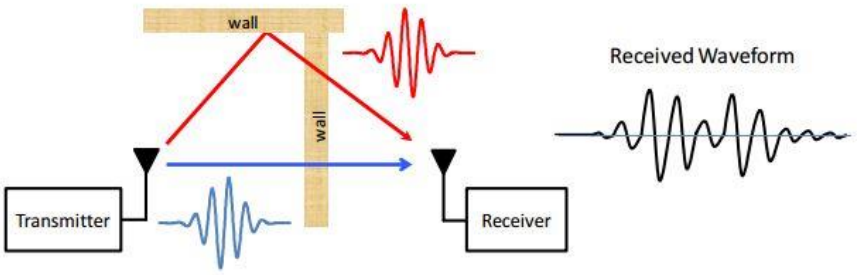


**Figure 2: Multipath in a cluttered environment. The transmitted pulse is shown in blue, reflected pulse in red and received pulse in black. (After White paper: Time Domain P410 UWB).**

As seen in the above figure, red pulse is the reflected pulse and transmitted pulse is shown in blue. The pulse received at the receiver is a combination of both and is shown in black colour. It is to be noted that the red pulse takes longer to arrive than the blue pulse and hence can be isolated at the receiver. Narrow band systems on the other hand cannot resolve this multipath because their pulses are too long resulting in an overlap between the transmitted and reflected pulses and hence cannot separated from each other. A typical example of a signal received by a UWB receiver kept in a cluttered environment is shown in Figure 3. The effect of multipath due to the environment is clearly seen in Figure 3.

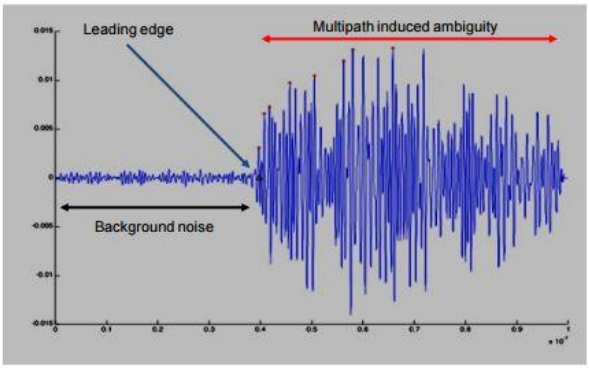


**Figure 3: Signal received by a UWB receiver kept in a cluttered environment. (After White paper: Time Domain P410 UWB)**

Since the actual (true) range between the UWBs is the straight path between the transmitter and receiver, it can be identified from the first pulse which arrives at the receiver which is referred to as the leading edge. However, from a practical perspective the precise location of the leading edge is ambiguous due to the noise resulting from multipath. This ambiguity in location of leading edge is less than one cycle of the RF signal which is equal to about 15 cm in range measurement. Using single processing algorithms, the range measurement ambiguity has been shown to reduce to less than 2mm (Petroff 2012). Thus, using two way TOF measurements and advanced signal processing algorithms for multipath mitigation, precise range measurements can be obtained using UWB.

### 2.1 Localization using range measurements

Once the range measurements from three or more UWB transmitters and/or Wi-Fi APs is available, the location of the platform (carrying UWB receiver and/or Wi-Fi receiver) can be determined using trilateration methods. This section explains this method of compute the

precise location using range measurements.

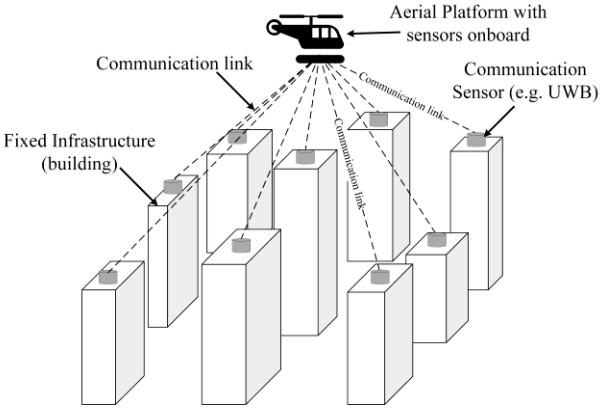


**Figure 4: A Cooperative P2I localization system (After Goel et al. 2016b).**

Consider a cooperative peer to infrastructure localization system as shown in Figure 4. A UWB receiver and/or Wi-Fi receiver is installed on the dynamic platform (UAV, car etc.). The relative range measurements from the fixed infrastructure to the platform are available. Further, the locations of the fixed infrastructure points are stored in a database on board the platform. Let range measurements from $m > 3$ infrastructure points (along with the corresponding coordinates) are available to the platform. Then following mathematical expressions can be written relating the range measurements, platform location and location of infrastructure points.

$$s_i = \sqrt{(x - x_i)^2 + (y - y_i)^2 + (z - z_i)^2} + \varepsilon_i,\ i = 1,2,....m; m > 3 \qquad \text{(Eq. 4)}$$

Where $\varepsilon_i$ denotes a random error in the range measurement with a known standard deviation. The above set of equations can be solved using least squares method of adjustment to compute the platform location. As is evident from the above equations, the quality of the computed solution is dependent on the quality of range measurements and relative location of the infrastructure points with respect to the platform. To achieve the platform location with good accuracy, large number of infrastructure points should be utilized and all the points should be well spread out with respect to the platform. The effect of relative location of the infrastructure points with respect to the platform will be demonstrated using numerical simulations in the later part of the paper.

## 3. MATHEMATICAL FRAMEWORK FOR COOPERATIVE LOCALIZATION

This section develops the mathematical framework for cooperative localization using UWB, Wi-Fi, GNSS and Inertial sensors such as gyroscopes and accelerometers. The heart of cooperative localization lies in the filtering and estimation technique used for fusion of information from different sensors. This paper uses Extended Kalman Filter (EKF) to fuse the measurements but other filters such as Unscented Kalman Filter (UKF) or Particle filter could also be used. The objective of the filter is to estimate the state of the dynamic platform (UAV, car, truck etc.) which includes position, velocity, attitude and sensor biases, thus making the state vector to be of size 16 and can be expressed as follows.

$$X = \begin{bmatrix} (r)^T & (v)^T & (\alpha)^T & (b_g)^T & (b_a)^T & c_b \end{bmatrix}^T \qquad \text{(Eq. 5)}$$

Where the superscript $T$ denotes the transpose. The notations $r$, $v$, $\alpha$, $b_g$, $b_a$ and $c_b$ denote the position, velocity, attitude, gyroscope bias, accelerometer bias and receiver clock bias respectively. The kinematic equations of motion for the dynamic platform in Earth Centred

Earth Fixed (ECEF) frame can be stated as follows. (Goel et al. 2016a).

$$\dot{r}^e = v^e \quad \text{(Eq. 6)}$$

$$\dot{v}^e = R_b^e f_b - 2\Omega_{ie}^e v^e + g^e \quad \text{(Eq. 7)}$$

$$\dot{\alpha}^e = R_{\alpha^e}\omega_{ib} \quad \text{(Eq. 8)}$$

Where $R_{\alpha^e}$ is given by:

$$R_{\alpha^e} = \begin{bmatrix} 1 & \sin\phi\tan\theta & \cos\phi\tan\theta \\ 0 & \cos\phi & -\sin\phi \\ 0 & \sin\phi\sec\theta & \cos\phi\sec\theta \end{bmatrix}$$

Where the position of a UAV in ECEF frame is denoted by $r^e$, UAV velocity is denoted by $v^e$, attitude vector is denoted by $\alpha^e$, skew symmetric matrix with respect to the inertial frame of earth rotation vector in ECEF frame is denoted by $\Omega_{ie}^e$, rotation matrix which transforms from IMU body to ECEF frame is denoted by $R_b^e$ and $f_b$ denotes the accelerometer observations. The biases in gyroscope, accelerometer and GNSS receiver clock are modelled using a random walk model and can be expressed as follows.

$$(b_g)_{k+1} = (b_g)_k + w_g^k \quad \text{(Eq. 9)}$$

$$(b_a)_{k+1} = (b_a)_k + w_a^k \quad \text{(Eq. 10)}$$

$$(c_b)_{k+1} = (c_b)_k + w_{c_b}^k \quad \text{(Eq. 11)}$$

Where $w^k$ denotes a random noise and is assumed to follow normal distribution with a given covariance. Using the above mentioned kinematic model, the state space model of the EKF can be arrived at as follows. The general expression representing the time evolution of the state is expressed as,

$$\dot{X} = f(X, u, w) \quad \text{(Eq. 12)}$$

Where $f$ denotes a non-linear function, $\dot{X}$ denotes the time derivative of state vector, $u$ denotes the control input and $w$ denotes the random noise. The above non-linear model is linearized about an optimal state $X_o$ using Taylor series expansion. The resulting discretised version of the time evolution of state can be then be represented as,

$$X_{k+1} = F_k X_k + (f(X_o) - FX_o)\Delta t + B_k u_k \Delta t + G_k w_k \quad \text{(Eq. 13)}$$

Where $\Delta t$ is the sampling time, $F$ denotes the Jacobian with respect to state vector and $F_k = I + F\Delta t$. The matrix $F_k$ is called as the state transition matrix. The noise vector $w_k$ includes noise from accelerometer, gyroscope and receiver clock. The matrices $F_k$, $G_k$ and $B_k$ are given as follows.

$$F_k = \begin{bmatrix} I_{3x3} & I_{3x3}\Delta t & 0_{3x3} & 0_{3x3} & 0_{3x3} & 0_{3x1} \\ 0_{3x3} & (I_{3x3} - 2\Omega_{ie}^e \Delta t) & E\Delta t & -R_b^e \Delta t & 0_{3x3} & 0_{3x1} \\ 0_{3x3} & 0_{3x3} & I_{3x3} + D\Delta t & 0_{3x3} & -R_{\alpha^e}\Delta t & 0_{3x1} \\ 0_{3x3} & 0_{3x3} & 0_{3x3} & I_{3x3} & 0_{3x3} & 0_{3x1} \\ 0_{3x3} & 0_{3x3} & 0_{3x3} & 0_{3x3} & I_{3x3} & 0_{3x1} \\ 0_{1x3} & 0_{1x3} & 0_{1x3} & 0_{1x3} & 0_{1x3} & 1 \end{bmatrix} \quad \text{(Eq. 14)}$$

$$G_k = \begin{bmatrix} 0_{3x3} & 0_{3x3} & 0_{3x3} & 0_{3x3} & 0_{3x1} \\ R_b^e \Delta t & 0_{3x3} & 0_{3x3} & 0_{3x3} & 0_{3x1} \\ 0_{3x3} & R_{\alpha^e} \Delta t & 0_{3x3} & 0_{3x3} & 0_{3x1} \\ 0_{3x3} & 0_{3x3} & I_{3x3} & 0_{3x3} & 0_{3x1} \\ 0_{3x3} & 0_{3x3} & 0_{3x3} & I_{3x3} & 0_{3x1} \\ 0_{1x3} & 0_{1x3} & 0_{1x3} & 0_{1x3} & 1 \end{bmatrix} \quad \text{(Eq. 15)}$$

$$B_k = \begin{bmatrix} 0_{3x3} & 0_{3x3} \\ R_b^e & 0_{3x3} \\ 0_{3x3} & R_{\alpha^e} \\ 0_{3x3} & 0_{3x3} \\ 0_{3x3} & 0_{3x3} \\ 0_{1x3} & 0_{1x3} \end{bmatrix} \quad \text{(Eq. 16)}$$

Where $E = -\frac{\partial\left(R_b^e b_a\right)}{\partial \alpha^e}$, $D = -\frac{\partial\left(R_{\alpha^e} b_g\right)}{\partial \alpha^e}$ and $I$ denotes an identity matrix. Therefore, using the above mentioned equations, the time evolution of the state space can be computed. In the absence of any measurements from either GNSS, UWB or Wi-Fi, the time evolution of the state would continue resulting the error to grow and ultimately causing the filter due to diverge. This is due to the accumulation of errors in gyroscope and accelerometer observations. To keep the filter from diverging, measurements from at either GNSS, UWB or Wi-Fi is required. The pseudorange measurements obtained from GNSS while direct range measurements are available from UWB and range measurements can be computed from TOF measurements derived from Wi-Fi. The model for incorporating GNSS pseudorange measurements is given as,

$$\rho_p = \sqrt{\left(x_p - x\right)^2 + \left(y_p - y\right)^2 + \left(z_p - z\right)^2} + \left(c_b\right) + e_{\rho_p} \quad \text{(Eq. 17)}$$

Where $p$ denotes the satellite number and $e_{\rho_p}$ denotes the random error in the pseudorange measurement. It is to be noted that the receiver clock bias is unknown and forms a part of the state vector. The measurement model for range measurements derived from UWB and Wi-Fi is given by equation 4. Let pseudorange measurements from $p$ satellites and range measurements from $m$ UWBs and $n$ Wi-Fi APs is available. The complete measurement model can be written as,

$$Z_k = h\left(X_k\right) + v_k \quad \text{(Eq. 18)}$$

Where $h\left(X_k\right)$ is the non-linear measurement function and includes equations of the form given in equation (4) and (17). As before, the measurement model is linearized about the optimal state and the discretised measurement model (Goel et al. 2016a) is written as,

$$Z_k \approx H_k X_k + h\left(X_o\right) - H_k X_o + v_k \quad \text{(Eq. 19)}$$

Where $H_k$ denotes the Jacobian of the measurement function with respect to the state vector and evaluated at the optimal state and is called as the measurement matrix. In the case when measurements from GNSS, UWB and Wi-Fi are available, the measurement vector and measurement matrix is given as follows.

$$Z_k = \begin{bmatrix} \rho_1 & \rho_2 & . & . & \rho_p & s_1^U & . & . & s_m^U & s_1^W & . & . & s_{n-1}^W & s_n^W \end{bmatrix}^T \quad \text{(Eq. 20)}$$

$$H_k = \begin{bmatrix} \frac{\partial \rho_1}{\partial r} & 0_{1x3} & 0_{1x3} & 0_{1x3} & 0_{1x3} & 1 \\ . & . & . & . & . & . \\ \frac{\partial \rho_p}{\partial r} & 0_{1x3} & 0_{1x3} & 0_{1x3} & 0_{1x3} & 1 \\ \frac{\partial s_1^U}{\partial r} & 0_{1x3} & 0_{1x3} & 0_{1x3} & 0_{1x3} & 0 \\ . & . & . & . & . & . \\ \frac{\partial s_m^U}{\partial r} & 0_{1x3} & 0_{1x3} & 0_{1x3} & 0_{1x3} & 0 \\ \frac{\partial s_1^W}{\partial r} & 0_{1x3} & 0_{1x3} & 0_{1x3} & 0_{1x3} & 0 \\ . & . & . & . & . & . \\ \frac{\partial s_n^W}{\partial r} & 0_{1x3} & 0_{1x3} & 0_{1x3} & 0_{1x3} & 0 \end{bmatrix} \quad \text{(Eq. 21)}$$

Where $s_i^U$ and $s_i^W$ denote the range measurements from $i^{\text{th}}$ UWB transmitter and Wi-Fi AP, respectively. The length of the measurement vector in this case is $(m+n+p)$. It is evident that to prevent the filter from diverging, length of measurement vector should be greater than 4, i.e. $(m+n+p)>4$. In the absence of any of GNSS, UWB or Wi-Fi measurements, the corresponding rows from measurement matrix and measurement vector can be removed. Since the transition matrix and measurement matrix are now defined, the time update and measurement update of the state vector can be performed using the standard equations of Extended Kalman Filter.

## 4. RESULTS AND DISCUSSION

This section discusses the results of numerical simulations and presents the preliminary results of a prototype of a cooperative localization system. The effect on the resulting localization accuracy due to the use of UWB, Wi-Fi and GNSS alone and in conjunction is also studied. Further, this section discusses the effect of increasing the number of infrastructure points (either UWB or Wi-Fi) on the localization accuracy and how the accuracy is effected by UWB and Wi-Fi even in presence of GNSS signals.

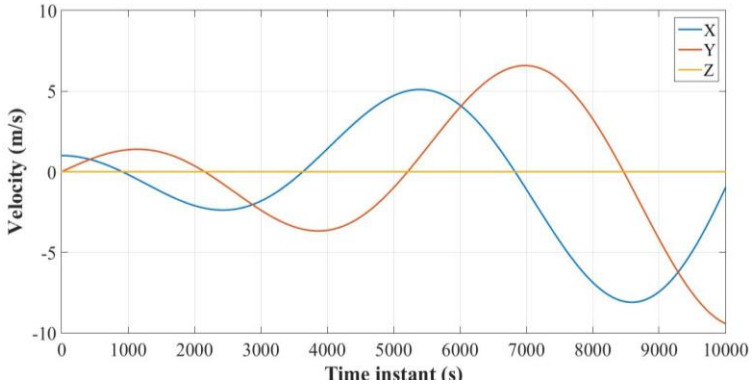


**Figure 5: Plot of true (simulated) velocity of the dynamic platform.**

This simulation considers a UAV equipped with GNSS, inertial sensors, UWB receiver and Wi-Fi. The GNSS is assumed to be accurate to about 4 m and ranging accuracy of UWB and Wi-Fi is assumed to be accurate up to 1 m and 5 m respectively. Although the UWB manufacturer has claimed the accuracy to be about 2 cm, it was rarely achieved by authors in a dynamic environment. In authors' experience, a ranging accuracy of 2 cm by UWB was achieved under ideal LOS conditions and static environments. This accuracy degraded to

about 1 m in dynamic environments although the exact estimates are difficult to be quantified. Literature shows that the best ranging accuracies achieved by Wi-Fi are of the order of 5 m (Schauer et al. 2013) and hence the same have been assumed in this simulation. A number of infrastructure points with known coordinates have been assumed to be present in the region surrounding the area of UAV operation. Figure 5 shows the dynamics of the simulated platform via a velocity plot. Figure 6 shows the simulated cooperative network with 10 infrastructure points available in the vicinity of the UAV. The lines show the communication between infrastructure point (Wi-Fi/UWB) and UAV. Figure 7 shows the RMS error in X and Y location of UAV operating in absence and presence of GNSS along with information provided by either UWB or Wi-Fi. As can be seen in Figure 7, the error is less when the number of infrastructure nodes is higher and when UWB measurements are used instead of Wi-Fi. The worst accuracy is achieved when Wi-Fi measurements (instead of UWB) are used and the number of infrastructure nodes available are less. The best accuracy is achieved when both GNSS and large number of UWB measurements are available simultaneously.

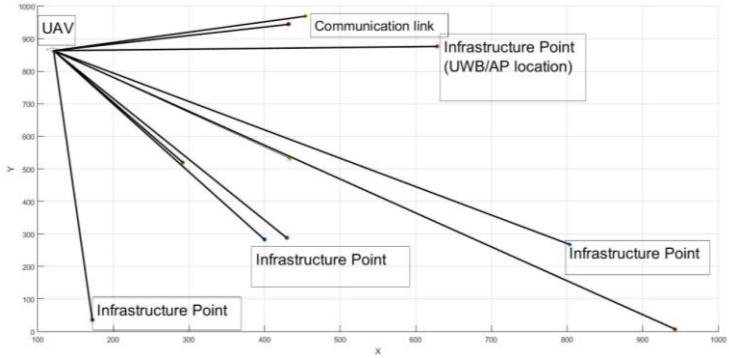


**Figure 6: An example of a cooperative network with 10 infrastructure nodes (Plan view).**

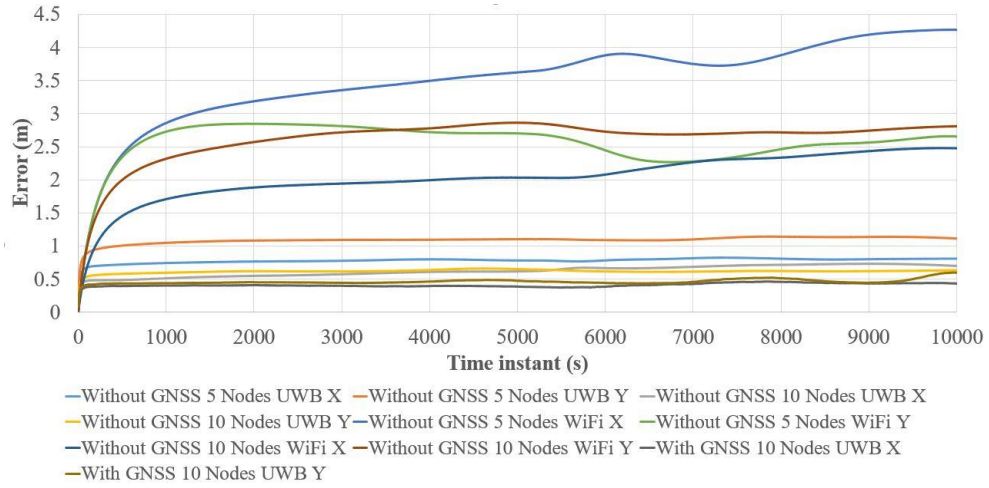


**Figure 7: RMS error in trajectory of platform along X and Y directions. It is assumed that GNSS is not present and either UWB or Wi-Fi aids the platform in localization.**

The prototype platform for cooperative P2I localization is shown in Figure 8. Sensors such as UWB, INS, GNSS and raspberry Pi are installed on the UAV along with an autopilot called 'Pixhawk'. The Inertial Measurement Unit (IMU) collects data at 50 Hz, GNSS collects data at 5 Hz while UWB is programmed to record observations at 100 Hz. An experimental setup for cooperative P2I localization is shown in Figure 9. In this experiment, 5 UWBs were used out of which only 4 were usable due to malfunctioning of one of the UWBs. The plot of UAV velocity in X, Y and Z as derived from GNSS measurements is shown in Figure 10. It is seen very clearly that UAV was very dynamic during the experiment with velocities ranging up to 3m/s. In this experiment, it is assumed that GNSS is not present at all and hence GNSS measurements are used as reference data. The localization of the UAV is done on the basis of

INS observations and UWB measurements. Figure 11 shows the availability of UWB measurements during the experiment. It is observed that more than 97% of the time of UAV operation, less than 3 UWB measurements were available and only 2.5% of the time, adequate number of measurements required for localization are available.

**Figure 8: Prototype cooperative localization UAV platform. UWB, GNSS and INS along with raspberry Pi is integrated on UAV.**

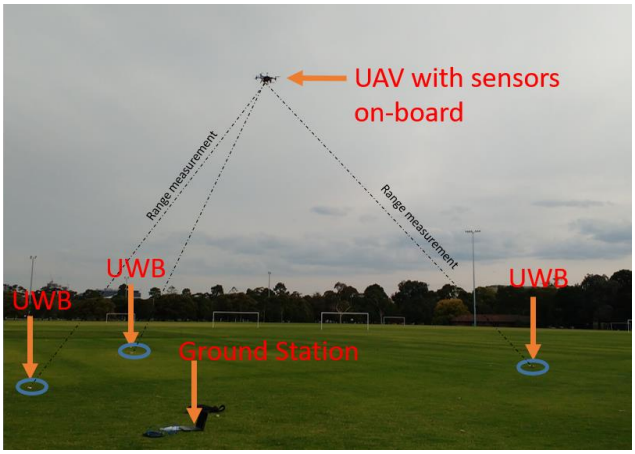


**Figure 9: Experimental setup of cooperative P2I localization.**

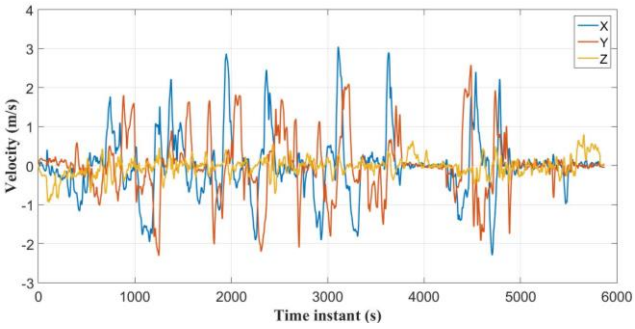


**Figure 10: Velocity plot of UAV during cooperative localization experiment.**

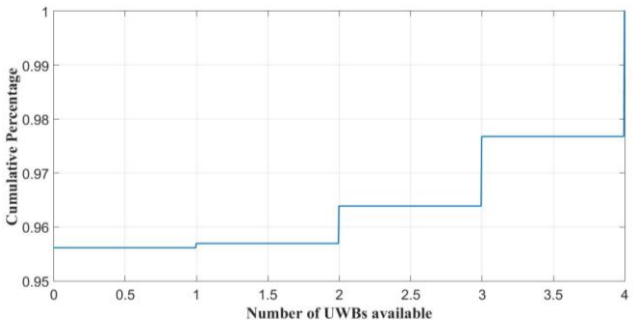


**Figure 11: Plot of availability of UWB measurements during the localization experiment.**

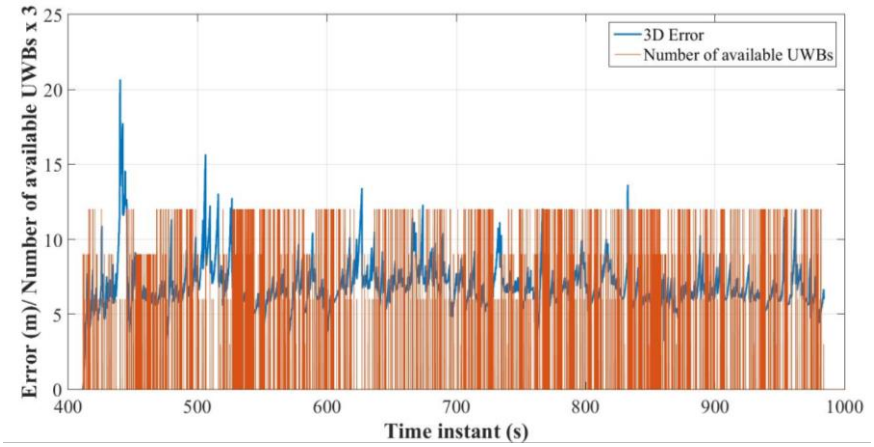


**Figure 12: Error plot (w.r.t GNSS) of UAV location with UWB availability overlaid.**

Figure 12 to Figure 14 show the results of the localization experiment. Figure 12 shows the error in derived UAV location with number of UWBs (scaled by a factor of 3) overlapped. A zoomed version of Figure 12 is shown in Figure 13. It is observed in Figure 12 and Figure 13 that the best possible accuracy is of the order of 5 m and is achieved when 4 UWB measurements are available for an extended period of time. When less than 3 UWB measurements are available, the error in UAV location starts to grow due to accumulation of

INS errors. When at least 3 UWB measurements are achieved, the error stabilizes around 8-10m. A plot of cumulative distribution of error in UAV location is shown in Figure 14.

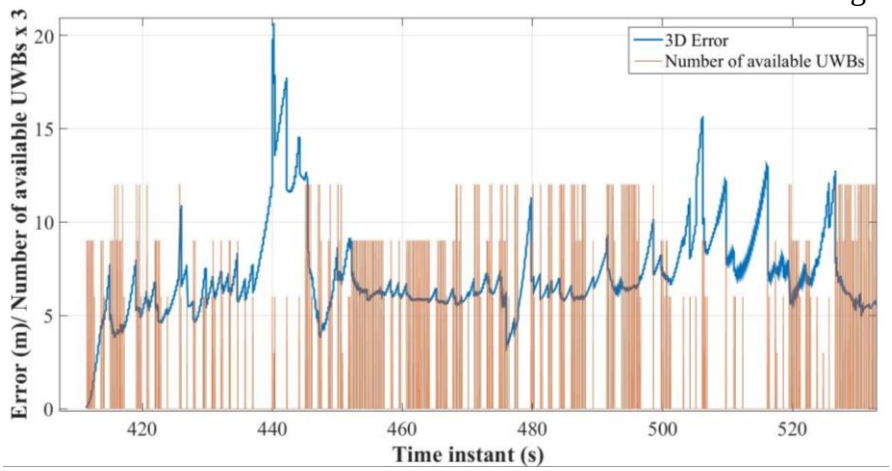


**Figure 13: Zoomed in view of Figure 12.**

It is evident that more than 95% of the time, the error in UAV location is less than 10 m and more than 85% of the time, the error is less than about 8 m. It is to be noted that this accuracy is obtained in pure GNSS denied regions and solution is dependent on the UWB measurements. More number of UWB measurements would further increase the location accuracy. In author's experience, increasing the number of UWB beyond 7 results in a localization accuracy of about 5m about 90% of the time which is quite a significant improvement.

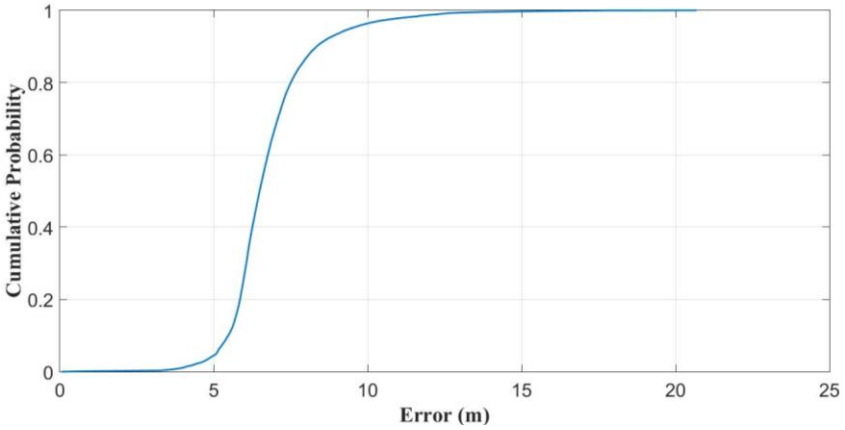


**Figure 14: CDF plot of error in UAV location.**

Further improvement in the localization accuracy can be achieved only if better quality UWB measurements are available and improved time synchronization of the sensors. Some of the major challenges which need to be resolved to achieve better localization include improved sensor synchronization, use of multi-channel UWB systems and improvement in quality of range measurements in dynamic environments.

## 5. CONCLUSIONS AND FUTURE WORK

This paper developed a cooperative P2I localization system using GNSS, INS, UWB and Wi-Fi including the mathematical framework for localization and a prototype of the system. The simulation results show that in the absence of GNSS signals, better accuracy is achieved using UWB measurements rather than Wi-Fi signals. This is due to availability of better TOF measurements in UWB as compared to Wi-Fi. Experiments were performed using the developed prototype using UWB measurements only. In GNSS denied regions, the developed prototype achieved an accuracy of less than 10 m, more than 95% of the time. In the case

when more than 4 UWB measurements are available for an extended period of time, the localization accuracy stabilized to about 5m. It is to be noted that this localization accuracy was achieved in absence of GNSS and when adequate (more than 3) UWB measurements are available only 2.5% of the time of operation. This paper demonstrated the feasibility of localization using UWB and Wi-Fi using state of the art systems. It can be concluded from this paper that current systems using UWB are capable of achieving accuracy up to 5 m. It is expected that accuracies resulting from Wi-Fi measurements would be poorer due to poor ranging accuracy. This has been validated by some authors in the literature (Schauer et al. 2013, Retscher and Tatschl 2016, Xiao et al. 2011) in the static environments. Future work would focus on more experimentation and evaluation of the developed system under different working conditions. Further, it is proposed to include a Wi-Fi receiver on board the UAV so as to include Wi-Fi measurements in the processing.

## REFERENCES


United Nations Report (2014) http://www.un.org/en/development/desa/news/population/world-urbanization-prospects-2014.html (Accessed September 30, 2016).

Schauer, L., Dorfmeister, F., Maier, M (2013) Potentials and limitations of WIFI-positioning using time-of-flight. *2013 International Conference on Indoor Positioning and Indoor Navigation, IPIN 2013*, (October), pp.28–31.

Retscher, G., Tatschl, T. (2016) Differential Wi-Fi – A Novel approach for Wi-Fi Positioning using Lateration. In *Recovery from Disaster, FIG Working Week 2016*, Christchurch, New Zealand, May 2-6, 2016.

Bailey, T., Bryson, M., Mu, H., Vial, J., McCalman, L., Durrant Whyte, H. (2011) Decentralised cooperative localization for heterogeneous teams of mobile robots, in Proc. of the IEEE International Conference on Robotics and Automation, Shanghai, China, pp. 2859-2865

Shi, X., Tiesheng, W., Huang, B., Zhao, C., (2010). Cooperative multi-robot localization based on distributed UKF. *Proceedings - 2010 3rd IEEE International Conference on Computer Science and Information Technology, ICCSIT 2010*, 6, pp.590–593.

Li, H., Nashashibi, F. (2013). Cooperative multi-vehicle localization using split covariance intersection filter. IEEE Intelligent Transportation Systems Magazine, 5(2), pp.33–44.

Wanasinghe, T.R., Mann, G.K.I., Gosine, R.G. (2014). Decentralized Cooperative Localization for Heterogeneous Multi-robot System Using Split Covariance Intersection Filter. In *2014 Canadian Conference on Computer and Robot Vision*. IEEE, pp. 167–174.

Goel S, Kealy A, Lohani B (2016a) Cooperative UAS localization using low cost sensors, *ISPRS Annals of Photogrammetry Remote Sensing and Spatial Information Sciences* III-1: 183-190, doi:10.5194/isprs-annals-III-1-183-2016.

Goel S, Kealy A, Lohani B (2016b) Infrastructure vs Peer to Peer Cooperative Positioning: A comparative analysis, *Proceedings of ION GNSS+ 2016*, Portland, Oregon, USA, September 12-16, 2016.

Julier, S.J., Uhlmann, J.K. (1997). A non-divergent estimation algorithm in the presence of unknown correlations. *Proceedings of the 1997 American Control Conference (Cat. No.97CH36041)*, 4, pp.2369–2373.

Hlinka, O., Sluciak, O., Hlawatsch, F., Rupp, M. (2014). Distributed data fusion using iterative covariance intersection. In *2014 IEEE International Conference on Acoustics, Speech and Signal Processing (ICASSP)*. IEEE, pp. 1861–1865.

Carrillo-Arce, L.C., Nerurkar, E. D., Gordillo, J. L., Roumeliotis, S. I. (2013). Decentralized multi-robot cooperative localization using covariance intersection. In *2013 IEEE/RSJ International Conference on Intelligent Robots and Systems*. IEEE, pp. 1412–1417.

Chen, X., Gao, W., Wang, J. (2013). Robust all-source positioning of UAVs based on belief propagation. *EURASIP Journal on Advances in Signal Processing*, 2013(1), p.150.

Savic, V., Zazo, S. (2013). Cooperative localization in mobile networks using nonparametric variants of belief propagation. *Ad Hoc Networks*, 11(1), pp.138–150.

Wan, J., Zhong, L., Zhang, F. (2014). Cooperative Localization of Multi-UAVs via Dynamic Nonparametric Belief Propagation under GPS Signal Loss Condition. *International Journal of Distributed Sensor Networks*, 2014, pp.1–10.

Savic, V., Poblacion, A., Zazo, S., Garcia M. (2010). Indoor Positioning Using Nonparametric Belief Propagation Based on Spanning Trees. *EURASIP Journal on Wireless Communications and Networking*, 2010(1).

Xiao, W., Ni, W., Toh, Y.K. (2011) Integrated Wi-Fi fingerprinting and inertial sensing for indoor positioning. In *2011 International Conference on Indoor Positioning and Indoor Navigation, IPIN 2011*.

Mok, E., Retscher, G. (2007) Location determination using WiFi fingerprinting versus WiFi trilateration. *Journal of Location Based Services*, 1(2), pp.145–159.

Husen, M.N., Lee, S. (2014) Indoor human localization with orientation using WiFi fingerprinting. *Proceedings of the 8th International Conference on Ubiquitous Information Management and Communication - ICUIMC '14*, pp.1–6.

Retscher G, Zhu M, Zhang K (2012) RFID Positioning. In *Chen R (ed.): Ubiquitous Positioning and Mobile Location-Based Services in Smart Phones*. Hershey PA, USA: IGI Global, 69-95.

Lanzisera, S., Zats, D., Pister, K.S.J. (2011) Radio frequency time-of-flight distance measurement for low-cost wireless sensor localization. *IEEE Sensors Journal*, 11(3), pp.837–845.

Li, X., Pahlavan, K., Latva-aho, M., Ylianttila, M., (2000). Comparison of indoor geolocation methods in DSSS and OFDM wireless LAN systems. *Vehicular Technology Conference, 2000. IEEE VTS-Fall VTC 2000. 52nd*, 6, pp.3015–3020 vol.6.

Yamasaki, R., Ogino, A., Tamaki, T., Uta, N., Matsuzawa, N., Kato, T., (2005). TDOA location system for IEEE 802.11b WLAN. In *IEEE Wireless Communications and Networking Conference, WCNC*. pp. 2338–2343.

Abusubaih, M., Rathke, B., Wolisz, A. (2007). A Dual Distance Measurement Scheme for Indoor IEEE 802.11 Wireless Local Area Networks. *Proceedings of the 9th International Conference on Mobile and Wireless Communications Networks*, pp.121–125.

Wong, C., Klukas, R., Messier, G. (2008). Using WLAN infrastructure for angle-of-arrival indoor user location. In *IEEE Vehicular Technology Conference*.

Petroff, A. (2012) A practical, high performance ultra-wideband radar platform. In *IEEE XNational Radar Conference - Proceedings*. pp. 0880–0884.

White Paper: Time Domain P410 UWB, http://www.timedomain.com/white-papers/320-0294B%20Time%20Domain's%20UWB%20Definition%20&%20Advantages.pdf (Accessed September 30, 2016).